Eur. J. Mineral.
1997, **9**, 763-783

Electron microprobe analysis and X-ray diffraction methods in archaeometry: Investigations on ancient beads from the Sultanate of Oman and from Sri Lanka

CORDELIA RÖSCH[1], RAINER HOCK[1], ULRICH SCHÜSSLER[1], PAUL YULE[2] and ANNE HANNIBAL[3]

[1]Mineralogisches Institut, Universität Würzburg, Am Hubland, D-97074 Würzburg

[2]Institut für Ur- und Frühgeschichte, Universität Heidelberg, Marstallhof 4, D-69117 Heidelberg, priv. Am Büchel 77, D-53173 Bonn

[3]Kommission für Allgemeine und Vergleichende Archäologie, Endenicher Strasse 41, D-53115 Bonn

Abstract: Beads from graves of the Samad Culture, Sultanate of Oman, and from an ancient craftsmen quarter of the old kingdom of Ruhuna, excavated in Sri Lanka, were investigated using electron microprobe analysis and X-ray powder diffraction. Both experimental methods were optimized towards a non-destructive analysis of archaeological finds. Based on their analysis, the beads from Oman can be divided into those made from natural rocks or minerals, metal, glass, Egyptian Blue and synthetic enstatite. Preferred natural rock types are serpentinite, chloritite and massive chlorite amphibolite which occur in the Samail Ophiolite of Oman and indicate a local production of these beads. Garnet beads are almandine-pyrope-rich and are interpreted as imports from the Sri Lanka/India area. Metal beads are made from pure Ag, ± pure Au or from Ag-Au-Cu alloys. Reddish-brown glass beads from Oman are Na-rich and coloured by Cu present in the glass matrix. Opaque red glass beads from Sri Lanka are commonly K-rich and coloured by tiny cuprite droplets which recrystallized from the melt and which are intensively disseminated within the glass matrix. Blue-white-blue and brown-white-brown sandwich beads from Oman and Sri Lanka are stylistically similar, but differ in composition of the white glass. Parts of the glass beads from Oman is partially or completely altered to form smectite. A cogged wheel bead from Oman was cut from steatite and then hardened by transformation of the steatite to synthetic enstatite during firing at about 1000°C. Large amounts of microbeads from a Samad grave also consist of synthetic enstatite and most probably were produced from Mg-rich clay by firing. Comparable beads have been recovered from excavations in the Indus area, especially Harappa, but also in the Arabian Emirates.

Key-words: archaeometry, beads, Oman, Sri Lanka, glass weathering, Egyptian Blue.

Introduction

One hundred years ago, on the 8th of November 1895, X-rays were discovered by Wilhelm Conrad Röntgen at the University of Würzburg. From that time on, a wealth of analytical methods has been developed that use X-rays to obtain a wide range of information about quite different materials. During the last three or four decades, X-ray powder diffraction and electron microprobe analysis have become common tools for structural and microchemical investigations in

0935-1221/97/0009-0763 $ 5.25

modern material sciences, crystallography, mineralogy and petrology. Their use in archaeology, however, is still more or less sporadic, although these methods allow non-destructive or nearly non-destructive analysis of archaeological finds. They can contribute to the unequivocal identification of materials used for the fabrication of ancient objects that cannot be worked out by archaeological investigations alone.

The 100th anniversary of the discovery of X-rays serves as an occasion to demonstrate the versatility of X-ray powder diffraction and electron microprobe analysis to characterize the materials used by earlier cultures. In this paper we focus on examples taken in the context of our current archaeometric projects which deal with Pre-Islamic beads from the Sultanate of Oman and with beads from old Singhalese kingdoms in Sri Lanka (for locations see Fig. 1). The significance of the data for further interpretations concerning technology of bead fabrication and origin of beads is discussed.

Archaeological background

For the past twenty years, excavations in the Sultanate of Oman have been undertaken regularly by archaeologists under the aegis of the German Mining Museum in Bochum. The initial intent of this research project was to gain insight into the more than 5000-years-old copper mining and smelting activity in this region (Hauptmann, 1985). In addition, ancient settlements and cemeteries were uncovered, which helped to elucidate Oman's Pre-Islamic cultures. In 1980, a previously unknown, non-writing, Iron Age culture was discovered at the oases of al Maysar and Samad al Shan and therefore was named the Samad Culture (300 BC - 900 AD; Yule, 1992, 1993, 1994). This culture became the emphasis of the excavations from 1987 to 1991. Beside iron weapons, bronze vessels, and a hitherto unknown kind of handmade ceramic pottery, about 8000 beads fashioned from diverse materials were recovered from graves of the Samad Culture. Some of the beads derive from find contexts as early as 3000 BC.

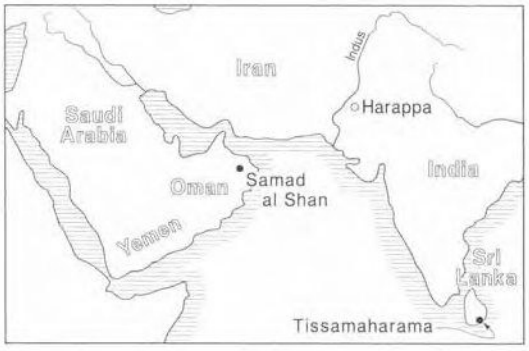

Fig. 1. Geographic position of the excavation sites Samad al Shan in the Sultanate of Oman and Tissamaharama in Sri Lanka. In Harappa, synthetic enstatite beads comparable to those from Samad were found (see discussion of archaeological aspects).

A series of beads representative of the different Pre-Islamic Periods in the Sultanate was selected for material analysis, including typical materials and problematic identifications. The data serve as a basis for a correct classification of the beads and provide information about the raw material and technology used for bead production. Of primary interest is the provenance of the beads. From the excavations, no evidence for local bead or glass production during the Samad Culture has yet been found. Material analysis could help to decide if raw materials were locally available, or if beads were imported, and if so, where from. Did the cultures of central Oman have an art industry of their own, or did they merely purchase objects and materials? When correlated with time, material analysis can point out classes of materials that may have been preferred in the different cultural periods.

Comparisons with beads from Sri Lanka proved useful in certain cases. These beads derive from excavations in Tissamaharama, which have been carried out since 1992 by the Commission of General and Comparative Archaeology, Bonn, and the Archaeological Department of Sri Lanka (Weisshaar & Wijeyapala, 1993, 1994). Subject of the excavations are relics of the settlement Mahagama, which was the capital of the kingdom of Ruhuna from the third century BC on. Ruhuna was the southeasternmost of the ancient Singhalesian kingdoms. At the southern end of a large hill measuring 600 x 200 metres, a part of the excavated settlement called Akurugoda, furnaces from ancient copper and bronze processing came to light, together with slags, moulds, abundant pottery fragments and more than 3600 beads made from different materials. Analytical investigations were started on a representative selection of these beads.

Analytical methods

Electron microprobe analysis

Chemical compositions of the beads were determined using a CAMECA SX50 electron microprobe with wavelength-dispersive spectrometers. The high spatial resolution of about 1-3 μm^3 allows non-destructive *in situ* analysis of archaeological finds, if certain prerequisites are satisfied.

The bead must be placed into the microprobe as a whole. A special sample-holder was constructed which allows the insertion of samples as large as 40 x 55 x 18 mm into the vacuum chamber. Accurate quantitative analysis can only be achieved for clean and polished sample surfaces. A mild and inconspicuous polishing is often necessary, but seldom affects the appearance of the beads. If the beads are badly corroded, the corrosion products must be locally removed. However, the method only probes near-surface regions of the sample. If the bulk of a bead is made of several layers of different materials, it is necessary to cut a cross-section to achieve a complete analysis of all layers. A destructive sample preparation is then unavoidable.

An essential requirement for the analysis of archaeological finds is the backscattered electron scanning image of the object. Microscopically small chemical inhomogeneities can be detected and subsequently analyzed.

Operating conditions were 15 kV accelerating voltage, 15 nA beam current and 1-2 µm beam size. For glass beads, a beam size of 20 µm was used to avoid thermally induced diffusion of alkali elements during analysis. Element peaks and backgrounds were measured with counting times of 20 s each; for Fe, Cu and Co, 30 s were chosen. Synthetic silicate and oxide minerals or pure elements were used as reference standards. Matrix correction was calculated by the PAP program supplied by CAMECA. An analytical error of less than 1% relative for major elements is verified by measurements on the respective standards. For low element concentrations, the analytical uncertainty increases. Using these operating conditions, the detection limit is at about 0.05 to 0.1 wt.% .

X-ray diffraction analysis

Part of the beads consist of monocrystalline or polycrystalline material. Glass beads sometimes contain crystalline components which give them a special appearance. X-ray powder diffraction serves for qualitative analysis of crystalline phases and gives information about the crystal structure and the state of crystallinity of the sample. Modern techniques of data analysis such as whole powder pattern fitting methods with or without *a priori* structural information can yield this information (Rietveld and Pawley methods: Pawley, 1981; Young, 1993). X-ray powder diffraction is especially useful where grain sizes are too small to allow unambiguous identification by electron microprobe, or in cases where materials of the same chemical compositions occur in different structural modifications.

Usually the method is destructive, but can still be applied whenever a single piece from a large collection of similar beads can be sacrificed for analysis, or when beads were broken in any case. Some beads are unique and must be preserved in their original state. In order to prevent damage to them, the diffraction experiment requires the construction and use of special sample holders. An almost flat surface segment of the bead must be brought onto the focussing circle of the diffractometer to keep aberrations of the 2θ-values and of reflection intensities as small as possible. Only a precise determination of d_{hkl}-values ensures a successful automated qualitative phase analysis by standard search/match procedures. The main problem is to get reliable diffraction data from beads of more or less irregular shape. The most frequently encountered bead shapes are barrels, spheres, cylinders, cones and discs. Certain bead shapes are already well-suited for diffraction experiments and exhibit a flat surface segment. Examples are the faces of discs and the basal planes of cylinders or of truncated cones. These beads are fixed onto a sample mount which is adjustable in height. Fig. 2a shows the sample mount with a disc-shaped bead in place. To irradiate only the flat part of the sample with the primary beam, the width of the horizontal aperture is chosen to match the lateral dimension of the bead.

For spheres or cylinders or, more generally, for objects of high surface curvature, the experimental situation is more complicated. Curved surfaces give rise to an enhanced peak asymmetry and to a shift of the peak positions. The problem can partly be overcome by use of a small horizontal aperture of about 1 mm. Only surface elements near the focussing circle are then used for diffraction. In this case, the irradiated sample

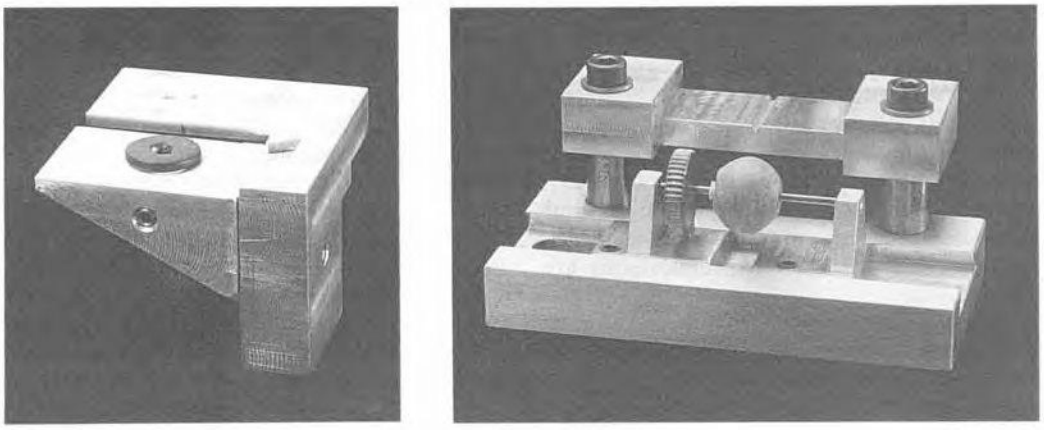

Fig. 2. **a**. A sample mount which is adjustable in height for non-destructive x-ray powder diffraction measurements. A flat surface segment of a bead can be adjusted onto the focussing circle of the diffractometer. **b**. Height-adjustable spinning device for non-destructive x-ray powder diffraction measurements of cylindrical and spherical beads. The rotation axis is mounted on ruby bearings and driven by an air stream blown onto the small paddle wheel.

volume is small and the powder statistics may become poor. Moreover, the diffraction pattern may not be representative of the phase content of the bead, because only a small part of the object is investigated. To reduce these experimental shortcomings, we rotate spherical and cylindrical beads around an axis through their threadhole. At each sequential counting step, the diffracted intensity is integrated over a few turns. Fig. 2b shows the spinning device with a spherical bead fitted. The rotation axis is mounted on ruby bearings and driven by an air stream blown onto a small brass paddle-wheel. By regulating the air flow, the number of revolutions per second is easily varied.

For all measurements we use Philips powder diffractometers PW1710 with or without a secondary monochromator. Operating conditions are 40 kV accelerating voltage and 30 mA beam current on a copper anode. The actual collimation of the primary beam depends on the shape of the bead and the size of the nearly flat surface segment which can be brought on the focussing circle. It varies from 0.5 to 1.0° vertical divergence and from 15 mm down to 1 mm horizontal beam widths. Diffractograms are taken in increments of 0.02° with typical counting times of 1 to 10 s. Long counting times are used in the identification of trace phases, where up to 5 repeated measurements with counting times of 2 s/step are summed up. For the phase analysis, the program JADE+ with ICDD data bank is used. Rietveld refinements of single phases or phase mixtures are done with the program of Hill & Howard (1986), based on the program by Wiles & Young (1981).

Materials used for bead production

Based on the different materials used for their production, the following groups of beads have been distinguished up to now (Rösch, 1994):
(1) Beads made from natural rocks or minerals: ultramafic rocks, garnet,

Fig. 3. **a**. Bead from a Samad grave made from chloritite, 5 mm diameter. **b**. One garnet bead typical for the finds in Samad as well as Tissamaharama; diameter 4.5 to 5 mm. **c**. Strongly corroded bispherical metal bead from a Samad grave, soldered together from two pure Ag spheres and a cylindrical connection made of an Ag-Au-Cu alloy; length 8.5 mm. **d**. Detail of a collier of golden pendants and spherical beads from Samad; length of the pendants about 9.5 mm. **e**. Flat, disc-shaped beads from Tissamaharama, made from opaque red copper glass; diameters 9 - 10 mm. **f**. Cuboid-shaped, blue sandwich glass bead with an opaque, white interlayer, recovered from a Samad grave; length 5 mm. **g**. This bead made from Egyptian Blue was a unique find of this material in Samad; diameter 5 mm. **h**. Numerous microbeads of synthetic enstatite from the Umm an-Nar Period were found in quantity in a Samad grave; diameter of the cylindrical beads range from 2.5 to 3 mm.

Fig. 3

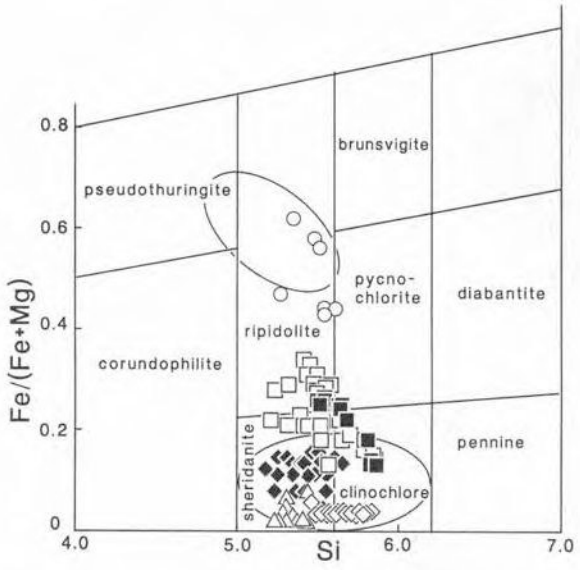

Fig. 4. Sheridanite/clinochlore and ripidolite compositions were found for chlorites forming the predominant mineral phase of six beads made of chloritite and massive amphibole-chlorite rock (each signature refers to one bead). Similar compositions (elliptical fields) were determined by David *et al.* (1990) for chloritites of other Oman archaeological finds as well as for chloritites from natural black-wall occurrences in the Oman Samail Ophiolite. Nomenclature from Hey (1954).

calcite/aragonite, SiO_2-varieties such as carnelian and chalcedony.
(2) Metal beads: Au, Ag, alloys of Au ± AgCu.
(3) Glass beads: alkali-silicate glass, lead glass, opaque red copper glass.
(4) Egyptian Blue beads.
(5) Synthetic enstatite beads

Selected examples of detailed material characterization and a discussion of some archaeological implications are given in the following.

Beads made from ultramafic rocks

Soft ultramafic rocks such as serpentinite, steatite, chloritite or massive chlorite-amphibole rock can easily be carved and therefore have been used preferentially for the production of ornaments in ancient cultures. These different kinds of rock are difficult to distinguish macroscopically. Non-destructive determination of the mineral assemblage and the chemical composition of the different minerals by microprobe analysis allows a detailed characterization of the rocks used for bead production. From the graves of the Samad Culture, several beads fashioned from these kinds of rocks were identified in the laboratory (for example Fig. 3a). According to the nomenclature of Hey (1954), the compositions of chlorites scatter within the more Mg-pronounced fields of clinochlore/sheridanite or within the somewhat more iron-rich ripidolite field (Fig. 4). Chlorites of the massive chlorite-amphibole rock are similar in composition to those from the chloritite. Amphiboles range between actinolite and actinolitic hornblendes in composition (Fig. 5), following the nomenclature of Leake (1978).

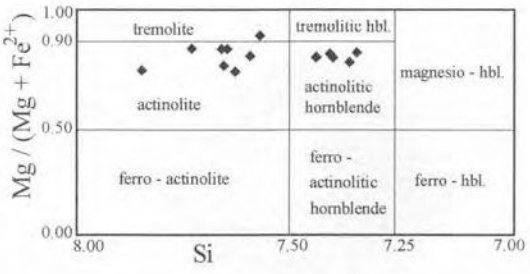

Fig. 5. Composition of amphiboles which form a major mineral phase of one bead made of massive chlorite-amphibole rock. Nomenclature from Leake (1978).

Table 1. Microprobe analyses of garnet beads from Samad/Oman (1-6), one garnet bead from Tissamaharama/Sri Lanka (7) and two garnet fragments from Tissamaharama (8, 9).

	Samad						Tissamaharama		
	1	2	3	4	5	6	7	8	9
wt.-%									
SiO_2	39.62	39.25	39.19	39.69	39.63	39.59	39.61	39.56	39.91
TiO_2	<0.1	0.12	<0.1	<0.1	<0.1	<0.1	<0.1	0.11	<0.1
Al_2O_3	21.98	21.73	21.45	22.04	21.94	22.05	22.15	22.13	22.38
Cr_2O_3	<0.1	<0.1	<0.1	<0.1	<0.1	<0.1	<0.1	<0.1	0.11
Fe_2O_3*	1.23	1.38	1.19	1.24	0.80	0.91	0.55	0.79	0.37
MgO	11.93	10.00	10.70	11.61	13.00	11.71	10.27	11.76	11.3
CaO	5.43	6.06	4.90	4.27	3.92	3.73	4.61	4.32	4.12
MnO	0.91	1.15	1.16	1.16	0.83	1.83	0.6	1.27	1.19
FeO	18.66	20.65	20.42	20.54	18.46	20.13	22.68	19.84	21.22
Total	99.76	100.34	99.01	100.55	98.58	99.95	100.47	99.78	100.60
Cations (O=24)									
Si	5.956	5.950	5.990	5.957	5.988	5.969	5.985	5.965	5.988
Al	0.044	0.050	0.010	0.043	0.012	0.031	0.015	0.035	0.012
Total	6.000	6.000	6.000	6.000	6.000	6.000	6.000	6.000	6.000
Ti	0.009	0.014	0.009	0.005	0.008	0.009	0.005	0.013	0.002
Al	3.851	3.831	3.854	3.854	3.896	3.887	3.931	3.898	3.945
Cr	0.007	0.004	0.001	0.007	0.006	0.004	0.002	0.003	0.012
Fe^{3+}	0.139	0.157	0.137	0.141	0.091	0.104	0.063	0.090	0.041
Total	4.006	4.006	4.001	4.007	4.001	4.004	4.001	4.004	4.000
Mg	2.673	2.261	2.438	2.596	2.928	2.632	2.313	2.644	2.527
Ca	0.874	0.984	0.803	0.687	0.634	0.602	0.746	0.698	0.662
Mn	0.116	0.148	0.150	0.148	0.106	0.233	0.077	0.162	0.151
Fe^{2+}	2.346	2.618	2.609	2.578	2.332	2.539	2.866	2.502	2.663
Total	6.009	6.011	6.000	6.009	6.000	6.006	6.002	6.006	6.003
Total	16.015	16.017	16.001	16.016	16.001	16.010	16.003	16.010	16.003
mol.-%									
Andradite	3.7	4.3	3.6	3.6	2.5	2.8	1.7	2.6	1.1
Grossular	10.7	12.0	9.7	7.6	8.0	7.1	10.7	9.0	9.7
Almandine	39.1	43.6	43.5	43.0	38.9	42.3	47.8	41.7	44.5
Spessartine	1.9	2.5	2.5	2.5	1.8	3.9	1.3	2.7	2.5
Pyrope	44.5	37.7	40.6	43.3	48.9	43.9	38.5	44.1	42.2

*Fe_2O_3 calculated approaching an ideal site-occupancy of 6, 4, 6

Garnet beads

In two graves of the Samad Period, a total of nine garnet beads in gemstone quality came to light (example in Fig. 3b). Chemical compositions of these beads were determined by non-destructive microprobe analysis with seven measurements per bead (selected analyses in Table 1). All of these beads possess very similar almandine-pyrope-dominated compositions with almandine 38 to 44 mol.% and pyrope 37 to 49 mol.%. Additionally, a subordinate grossular component between 5 and 13 mol.% was observed (Fig. 6).

In Tissamaharama, Sri Lanka, an ancient craftsmen quarter currently is under investigation. During the excavations, four garnet beads and several pieces of raw garnet used for bead production were recovered in layers dated from the 3rd to the 5th century AD (the dating is provisional, ^{14}C determinations are still pending). The chemical compositions of the beads were compared with those of the Samad beads (Table 1). With almandine 37 to 48 mol.%, pyrope 34 to 46 mol.% and grossular 8 to 15 mol.%, these garnets closely match the composition of the Oman garnet beads (Fig. 6).

Metal beads

The metal beads investigated are hollow spheres, sometimes crowned by granulated

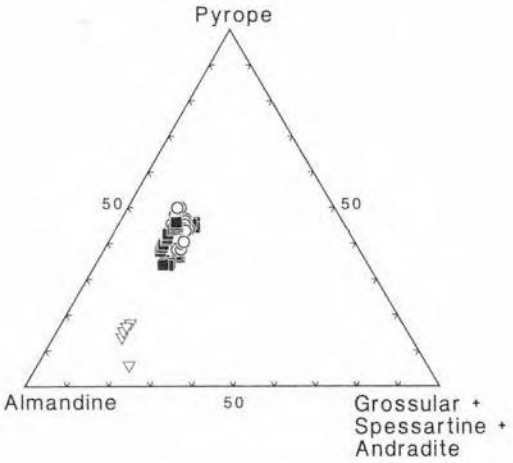

Fig. 6. End-member composition of nine garnet beads from two Samad graves (open circles represent 63 microprobe measurements). The composition of four beads and two pieces of raw garnet from the excavations of Tissamaharama are given by black squares (42 measurements). Open triangles mark the composition of garnets from Oman eclogites (El Shazly *et al.*, 1990).

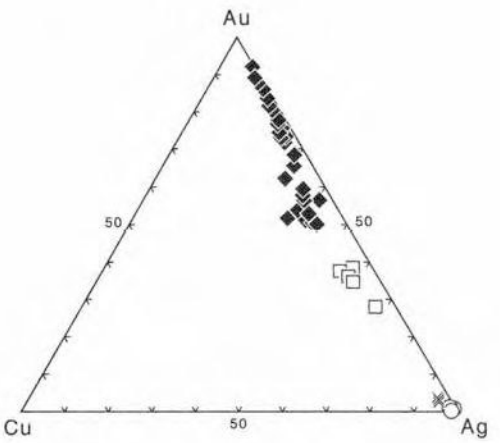

Fig. 7. Composition of the metal beads from Samad (wt.%, normalized to 100). Open circles: pure Ag single beads and spheres from the bead shown in Fig. 3c. Crosses: Ag-rich alloy with minor amounts of gold and copper, forming single beads. Open squares: Ag-Au-Cu alloy used for the cylindrical connection of the bead shown in Fig. 3c. Solid diamonds: Au-rich alloy with variable amounts of Ag and Cu, determined for beads and pendants of a golden collier recovered from one of the Samad graves (Fig. 3d).

smaller spheres. They are often badly corroded. Therefore, completely non-destructive analysis is not always possible. By polishing or cutting, an uncorroded metal surface suitable for microprobe analysis can be prepared. Results are shown in Fig. 7; selected analyses are given in Table 2. The beads consist of either pure Ag or Ag-rich alloys with small amounts of Au (3-4 wt.%) and Cu (1-2 wt.%).

A rare kind of metal bead is a combination of two spheres, joined by a short cylinder (Fig. 3c). Microprobe analysis of one of these beads shows that the spheres were made from pure Ag, whereas the cylindrical connection consists of an Ag-Au-Cu alloy with 54 wt.% Ag, 34 wt.% Au and 5 wt.% Cu, on the average (Fig. 7, 8; Table 2). The bead was not manufactured in one process, but rather the single parts were produced separately and then soldered together. Rapson (1990) describes the variation of colour of different alloys in the Au-Ag-Cu system, using an Au-Ag-Cu compositional triangle diagram. From this triangle, the original colour of the spheres is estimated as whitish, whereas the bond was whitish

Table 2. Microprobe analyses of various metal beads from Samad/Oman.

	1	2	3	4	5	6	7	8
Cu	0.1	6.4	0.0	1.6	0.2	1.3	2.0	4.2
Ag	99.1	53.2	89.3	94.5	99.8	11.0	18.3	28.1
Au	0.2	35.9	0.0	3.4	0.0	86.3	77.8	67.1
Cl	0.2	0.1	9.8	0.1	0.3	0.0	0.0	0.0
Total	99.6	95.6	99.1	99.6	100.3	98.6	98.1	99.4

Analyses 1-3 refer to the bispherical bead shown in Fig. 3c, with (1) and (3) measured on the two spheres and (2) taken from the cylindrical connection. An enhanced Cl content in (3) is the result of a progressive alteration during storage of the bead in the soil. Analyses (4) and (5) represent one silver-dominated and one pure silver bead. (6-8) give compositions of golden pendants as shown in Fig. 3d.

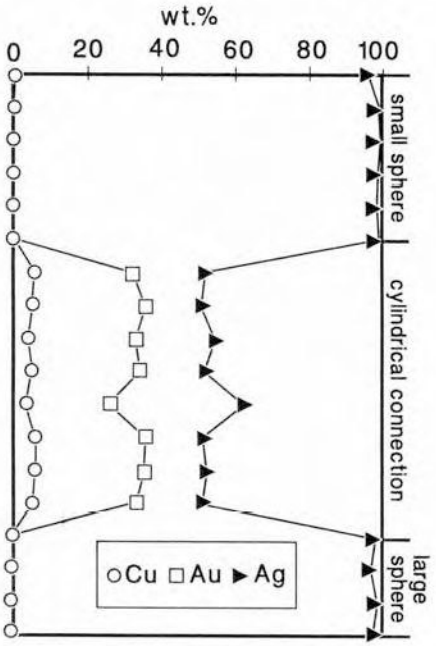

Fig. 8. Concentration profile for Ag, Au and Cu along the bispherical metal bead from Samad shown in Fig. 3c.

to greenish/yellowish. The bead certainly was strikingly attractive before it corroded.

Among the most spectacular finds from the Samad Period is a collier of golden pendants and spherical beads. The pendants are soldered together from a larger and a smaller hollow sphere along a join which is ornamented by a circle of still smaller golden spheres (Fig. 3d). As the beads and pendants are unaffected by corrosion, three pendants could be investigated by non-destructive microprobe analysis. The objects consist of an Au-rich alloy containing additional Ag and Cu (Table 2). The compositional variation of these added elements ranges from 5.5 to 31.5 wt.% for Ag and from 0.5 to 8.5 wt.% for Cu (Fig. 7).

Glass beads

The glass beads from Samad form a very heterogeneous group with regard to their shape, colour, chemical composition as well as technique of manufacture. Two main glass compositions are distinguishable: Major elements of *alkali-silicate glasses* are SiO_2, CaO and Na_2O in highly variable ratios. Additionally Al_2O_3, MgO and K_2O were found in varying amounts. *Lead glasses* are not pure SiO_2+PbO glasses, but contain CaO, Na_2O and, in part, Al_2O_3 as further oxides. The lead glasses fall into two groups with PbO between 4 and 15 wt.% and between 35 and 40 wt.%, respectively. Instead of a complete description of all the glass beads investigated, a

Table 3. Microprobe analyses of a brown-white-brown and a blue-white-blue sandwich bead from Samad/Oman, a blue-white-blue one from Tissamaharama/Sri Lanka, two spherical reddish-brown beads from Samad and two disc-shaped reddish-brown beads from Tissamaharama.

	sandwich beads						reddish brown beads			
	Samad				Tissama-harama		Samad		Tissama-harama	
	brown	white	blue	white	blue	white				
wt.-%										
SiO_2	71.9	71.8	71.6	75.6	71.2	75.5	62.3	69.6	65.0	67.2
TiO_2	0.5	0.4	0.2	0.2	0.3	0.2	0.4	0.5	0.2	0.2
SnO_2	<0.1	6.6	<0.1	2.5	<0.1	<0.1	nd	nd	nd	nd
Al_2O_3	6.3	3.0	3.7	3.0	6.9	3.5	9.7	5.4	4.0	4.4
MgO	1.0	0.8	0.5	1.0	0.3	0.5	0.8	1.7	1.9	1.8
CaO	5.7	5.2	5.6	5.7	5.3	5.7	3.9	5.2	3.4	1.5
MnO	0.2	0.6	1.4	0.3	1.0	<0.1	<0.1	<0.1	0.2	<0.1
FeO	1.0	0.9	0.7	0.7	0.9	0.6	2.3	1.8	1.4	1.7
CuO	nd	nd	nd	nd	nd	nd	0.7	1.5	13.7	13.5
Na_2O	10.1	9.7	14.5	10.0	11.8	11.4	16.9	10.2	1.9	2.6
K_2O	3.3	1.8	1.0	0.9	1.2	1.0	2.0	3.5	7.3	5.4
SO_3	<0.1	<0.1	0.2	<0.1	<0.1	<0.1	0.3	<0.1	<0.1	<0.1
P_2O_5	nd	nd	nd	nd	0.2	0.3	nd	nd	1.6	0.7
Cl	0.8	1.0	0.9	1.2	1.0	0.9	0.5	0.7	nd	nd
Total	100.8	101.8	100.3	101.1	100.1	99.6	99.8	100.1	100.6	99.0

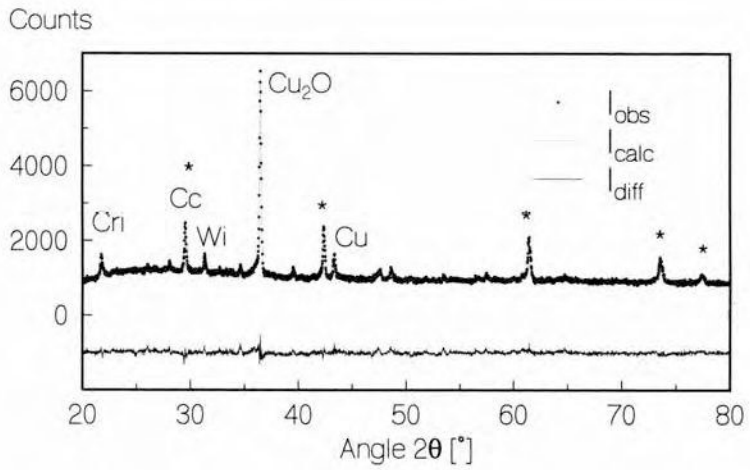

Fig. 9. X-ray powder diffractogram (non-destructive) of a disc-shaped bead (Fig. 3e) from Tissamaharama, made of opaque red copper glass. Cuprite was identified as the main crystalline component and refined together with the trace phases whitlockite, cristobalite, calcite and elementary copper by the Rietveld method. The strongest reflections of the four phases are indicated in the plot by Cri (cristobalite), Cc (calcite), Cu_2O (cuprite), Cu (copper) and Wi (whitlockite). asterisks mark subordinate reflections of Cu_2O. The main Cc reflection and one subordinate Cu_2O reflection are overlapping. Radiation was Cu-Ka.

comparison of reddish-brown opaque beads and of layered sandwich beads which were found in Samad as well as Tissamaharama is given here.

Reddish-brown opaque glass beads from Samad: These spherical or cylindrical beads are made of Na-dominated alkali-silicate glass (Table 3) or lead glass and are coloured by Cu-oxide (0.5-8 wt.% CuO), often in combination with Fe-oxide (about 1.5 wt.% FeO). By means of backscattered electron imaging, particles of Cu_2S with a typical size of a few microns were detected in one reddish-brown bead. Cu-sulphides obviously were taken for copper addition to the glass melt. The lack of sulphur in the glass matrix of most of the reddish-brown beads indicates that the copper sulphides were oxidized before adding to the melt, most probably by roasting. The observed Cu_2S particles may be relics of an incomplete roasting process.

Reddish-brown opaque glass beads from Tissamaharama: These flat, disc-shaped beads (Fig. 3e) were recovered from layers dated between the 3rd century BC and the 9th century AD. They are made from a K-dominated alkali-silicate glass with remarkably high Cu-contents of 10 to 15 wt.% (Table 3). Within this matrix, CaO- and P_2O_5-enriched patches have been detected. The whole matrix is intensively interspersed by numerous droplets of 1 to 10 µm in size, made visible by backscattered electron imaging. The droplets were identified as Cu-rich. Due to their small sizes, reliable quantitative microprobe analysis was not possible. In order to obtain more detailed information about the crystalline phases in the glass matrix, the beads were mounted on the height-adjustable sample holder and X-ray diffractograms were taken. Cuprite was identified as the main cristalline component. The minor phases elementary copper, whitlockite, calcite and cristobalite occur in highly variable amounts in different beads. As an example, Fig. 9 shows the measurement from one bead together with the result of a multiphase Rietveld refinement. Adjustable parameters in the fit were the scale factors and lattice constants of the individual phases, the zero point offset and the Pseudo-Voigt peak shape. A Caglioti function common to all phases was refined. The crystal structure data for the powder pattern calculation for cuprite, cristobalite and calcite were taken from Restori & Schwarzenbach (1986), Pluth *et al.* (1985) and Maslen *et al.* (1993) and kept fixed in the refinement. The background structured by the scattering from the amorphous glass phase was modelled phenomenologically by a 6th order polynomial.

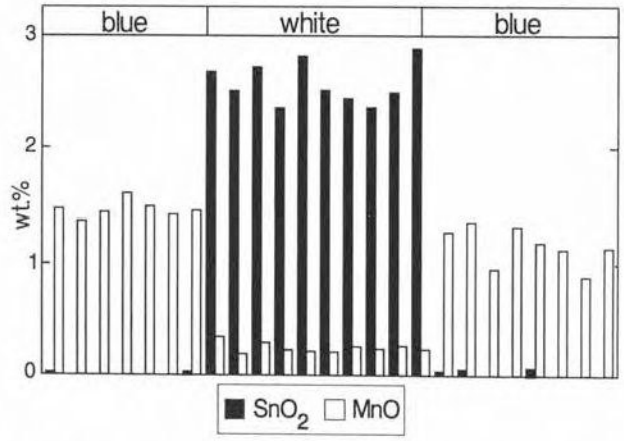

Fig. 10. Distribution of MnO and SnO_2 along a profile across the blue-white-blue sandwich bead from Samad shown in Fig. 3f.

Layered sandwich beads from Samad: These cuboid-shaped beads are usually translucent blue or brown, with one or two thin, white, opaque, layers in the middle (Fig. 3f).The sandwich beads are made from Na-dominated alkali-silicate glass (Table 3). The brown parts are coloured by addition of Fe, most probably occurring in it's trivalent state (Fe_2O_3 around 1 wt.% calculated from the microprobe analyses). The blue parts show conspicuously high MnO contents (around 1.3 wt.%), but also contain Fe, probably in the divalent state (FeO-contents around 0.7 wt.% calculated from the microprobe analyses). A light blue colour may be induced by a combination of the trace elements Mn and Fe, if the atmosphere during the melting process is reducing ($P_{O_2} \approx 10^{-9}$ bar; Sellner *et al.*, 1979). However, traces of Co, which were found in concentrations near the analytical detection limit of the microprobe, seem to be responsible for the intensive blue colour. SnO_2 contents of about 2.6 wt.% in a blue-white-blue bead and of about 7 wt.% in a brown-white-brown bead give the interlayers their white, opaque appearance. From backscattered electron imaging, a very inhomogeneous distribution of the Sn-content within the white interlayer became obvious. Fig. 10 reveals the concentrations of MnO and SnO_2 along a profile across a blue-white-blue sandwich bead.

Layered sandwich beads from Tissamaharama: Cuboid-shaped, blue-white-blue sandwich beads (dated around the 10th century AD) have a translucent, light blue matrix which is made of Na-dominated alkali-silicate glass. In composition it resembles that of the Samad sandwich beads (Table 3). Again it contains MnO (1 wt.%) and Fe (FeO-contents of 0.9 wt.%). These two elements may give the glass its blue colour in this case, since no contents of Co or further blue-colouring elements have been found. It should be noted that the blue sandwich beads have been chosen for laser ablation ICP mass-spectrometry to clarify the question of Co contents, which can colour a glass even if occurring in amounts below the detection limit of the microprobe. As opposed to those of the sandwich beads from Oman, the white interlayers do not contain any Sn. The reason for the white colour in these beads has not been found yet.

Numerous small patches of nearly pure P_2O_5 + CaO were detected by backscattered electron imaging in these beads. P_2O_5 and CaO contents of 42-43 wt.% and 54 wt.%, respectively, in the patches correspond rather exactly to an apatite composition and may result from former apatites which were concentrated as heavy minerals in the sands used for glass production. Other explanations for the occurrence of P and Ca in these beads include the addition of bone-ash to the melt.

Weathered glass beads

One group of beads from graves of the Samad Culture was classified during fieldwork as

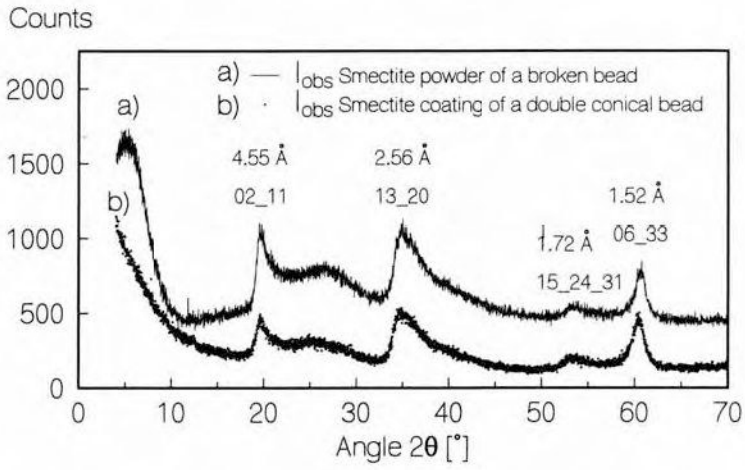

Fig. 11. X-ray powder diffractograms from saponite found to be the weathering product of glass beads from the Samad graves. Measurements of saponite powder recovered from a broken bead (solid line above) and a saponite layer covering an undestroyed, double conical bead (dots below) are compared. The most prominent hk-bands and corresponding lattice spacings are indicated. Radiation was Cu-Kα.

"fritte". This designates a kind of incompletely molten, loosely sintered glassy powder. From first microprobe and X-ray diffraction analyses it became clear that the material is actually more or less pure saponite, which belongs to the smectite group of clay minerals. Some beads consist entirely of smectite, others are coated with translucent smectite. Usually the transition between the glass core and the smectite coating is very sharp. Initially, these observations led to the interpretation that these beads form a separate group and the smectite was intentionally used as a raw material for the production of multilayered beads (Rösch, 1994). In the course of more detailed investigation, it became clear that smectite beads and coatings on glass beads represent an advanced stage of a weathering process which, up to now, has been rarely described for glasses in general.

Smectites most commonly occur as solid solutions of the Mg-, Fe- and Al-endmembers saponite, nontronite and beidellite (Brindley, 1980). Microprobe analyses yielded an almost pure saponite composition for the smectite coatings covering the Samad beads. A typical analysis, calculated on an oxygen basis of 10 and 2 OH groups, is:

$$(Na,K)_{0.12}Mg_{2.95}(Fe,Mn)_{0.07}[(OH)_2Si_{3.79}Al_{0.23}O_{10}].$$

The X-ray diffraction patterns (Fig. 11) confirm a pure smectite phase and compare well with those of sol-gel-produced synthetic saponites from studies of Strese & Hofmann (1941) and Grauby *et al.* (1993, 1994). Asymmetric (hk) reflections characteristic of a turbostratic stacking of layers are visible. Diffractograms measured on a powdered smectite coating obtained from a broken bead closely match the diffractogram non-destructively taken from an intact biconical bead covered by smectite.

Up to now weathering of man-made glasses to smectite has not been extensively studied. One solid phase of an about 5 µm thin alteration rim produced in the laboratory by hydrothermal alteration of an R7T7 simulated nuclear waste glass was identified as saponite (Abdelouas *et al.* 1995). Smectitic corrosion of naturally occurring glass spherules from the Cretaceous/Tertiary boundary has been described *e.g.* by Sigurdsson *et al.* (1991).

Varying degrees of alteration were observed for the corroded glass beads from Samad. Usually, smectitization starts from the surface of the beads and forms a clearly defined coating around a glassy core. This coating also occurs in the threadholes. The weathering process proceeds along small cracks into the glass core. During advanced corrosion of the bead, the glass is progressively replaced by smectite surrounding only a few irregular glassy relics. Interestingly, trace elements used for colouring of the glass may remain in the smectite coatings in comparable con-

centrations. For example, Co concentrations of 0.2 to 0.3 wt.% measured in the glassy core of a blue bead were also detected in the light yellow translucent smectite coating. Pb from a strongly altered lead glass bead was detected as well in the smectitic alteration layer.

Egyptian Blue beads

Egyptian Blue is a bluish synthetic material containing the blue calcium-copper tetrasilicate $CaCuSi_4O_{10}$ cuprorivaite (Pabst, 1959) and quartz as main constituents. The cuprorivaite and quartz crystals can be embedded in an alkali glass matrix yielding hard, semivitrified Egyptian Blue or may be loosely sintered crystallites leading to softer and more friable products. Egyptian Blue is produced by firing a mixture of quartz sand, calcium carbonate, a copper compound like malachite or copper-rich metal ingots (bronze filings), together with small amounts of alkali in a temperature range from 900° to 1100°C for several hours (Tite *et al.*, 1984; Jaksch, 1985; Noll, 1981, 1991). Depending on the raw materials used and the details of the manufacturing process, minor amounts of crystalline phases such as calcite, huntite, cassiterite, pyrite, crystobalite and Cu-wollastonite may occur (Noll, 1981; Jaksch, 1985).

Egyptian Blue was produced in Egypt from the third millennium BC onwards. From the beginning it was used in the fabrication of small art objects such as beads, and for the colouring of various ornaments. We investigated an Egyptian Blue bead from a Samad grave and a sample of this material from Qantir, lower Egypt, by means of powder diffraction. The powder diffractograms were refined by the Rietveld method.

The royal blue Omani bead (referred to as sample EB1) was a flattened sphere 5 mm in diameter, a height of 2.6 mm and a weight of 24 mg (Fig. 3g). Judging from the find context, this bead dates to the Lizq/Rumaylah (1200 - 300 BC) or the Samad Period (300 BC - 900 AD). Since diffraction experiments on the intact bead did not yield a data set refinable by the Rietveld method, half of the bead was prepared as a powder sample by grinding it in an agate mortar. The Egyptian Blue sample from Qantir (referred to as sample EB2) was retrieved as a compact powder in a small vessel. It was made available to us by T. Rehren of the German Mining Museum in Bochum. Its archaeological context dates to the Ramesside 20th dynasty, *i.e.* from 1200 to 1100 BC.

The powders were prepared on single-crystal quartz sample mounts in the form of stripes of 1 mm width and about 100 µm thickness. Measurements with two different orientations of the powder sample with respect to the incident beam were carried out. First, the sample was prepared as a 20 mm long stripe parallel to the incident beam direction, thus fitting the standard sample holder in length. The X-ray beam was collimated to 1/2° vertical divergence and a horizontal beam width of 2 mm. In the second experiment the sample was prepared as a powder stripe of 15 mm length orientated perpendicular to the primary beam. A vertical divergence of 1/2° and a horizontal beam width of 15 mm was used. This sample preparation provides enhanced reflection intensities at higher diffraction angles and is more suitable for the detection of weak reflections from trace phases.

The powder diagrams of sample EB1 basically show reflections from cuprorivaite and quartz. Trace phases were not detected except for a weak reflection at 30.3° which may be assigned to Cu-wollastonite. The X-ray diffraction pattern was evaluated by a two-phase Rietveld refinement of quartz and cuprorivaite. Starting values for the crystal structure data of cuprorivaite and quartz were taken from Pabst (1959) and Le Page & Donnay (1976). A total of 35 parameters was fitted. The global parameters include the scale factors, zero point shift, the peak shape parameters and the parameters of the Caglioti functions varied individually for both phases. A Pseudo-Voigt profile function was best fitted to the data. All refinements on both samples confirmed the crystal structure data for low quartz and this phase will not be discussed any further. For cuprorivaite (S.G. *P4/ncc*), the atomic coordinates of Ca, Cu, Si and O and the lattice parameters were refined. An isotropic temperature factor of 0.6 $Å^2$ (Pabst, 1959) was assigned to all atoms and kept fixed. The powder samples exhibit a pronounced preferred orientation which was accounted for in the calculation. The crystallite cleavage is perpendicular to [001] and the crystallite habit is platy. Similar degrees of preferred orientation were observed in both powders from Samad and Qantir for repeated sample preparations. A divergence slit correction was applied.

In sample EB2 from Qantir, three additional

Table 4. Atomic coordinates and cell parameters for cuprorivaite refined with the Rietveld method on two Egyptian Blue samples EB1 and EB2 from Samad/Oman and Qantir/Lower Egypt.

Cuprorivaite S.G. P4/ncc	perpendicular to primary beam 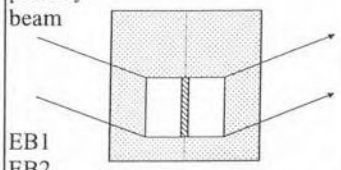 EB1 EB2			parallel to primary beam 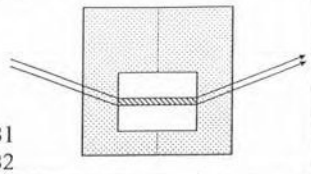 EB1 EB2		
atom coordinates	x	y	z	x	y	z
Ca 4b	0	0	0	0	0	0
Cu 4c	0.0	0.5	0.0821(2)	0.0	0.5	0.0819(3)
	0.0	0.5	0.0829(2)	0.0	0.5	0.0832(4)
Si 16g	0.2527(9)	0.1730(10)	0.1476(2)	0.2540(10)	0.1760(20)	0.1474(3)
	0.2560(10)	0.1750(10)	0.1477(3)	0.2510(20)	0.1790(30)	0.1456(6)
O_1 8f	0.2120(20)	0.2120(20)	0.25	0.2030(20)	0.2030(20)	0.25
	0.1960(20)	0.1960(20)	0.25	0.1990(30)	0.1990(30)	0.25
O_2 16g	0.4500(20)	0.2490(10)	0.1290(3)	0.4580(30)	0.2500(20)	0.1284(5)
	0.4440(30)	0.2490(20)	0.1338(5)	0.4470(50)	0.2640(30)	0.1314(9)
O_3 16g	0.1160(20)	0.2520(10)	0.0897(2)	0.1130(20)	0.2520(20)	0.0853(4)
	0.1120(20)	0.2570(20)	0.0852(4)	0.1140(30)	0.2310(30)	0.0820(6)
a, c [Å]	7.3104(3)	15.1347(4)		7.3100(4)	15.1327(6)	
	7.3099(3)	15.1372(4)		7.3120(6)	15.1305(8)	
η, G	0.570(60)	0.498(1)		0.460(10)	0.505(2)	
	0.640(4)	0.577(4)		0.600(20)	0.770(90)	
R-values						
R_{exp}	2.8			8.5		
	3.0			9.2		
R_{prof}	5.5			11.3		
	5.8			12.6		
R_{Bragg}	3.7			4.3		
	5.2			6.4		
GOF	8.6			3.0		
	7.3			3.1		

Preferred orientation, Pseudo-Voigt mixing parameter and residuals are given in addition.

trace phases cristobalite, cassiterite and calcite were identified and refined. Parameters identical to the ones used in the refinement of sample EB1 were varied for cuprorivaite. The crystal structure data for cristobalite, cassiterite and calcite were taken from Pluth *et al.* (1985), Baur (1956) and Maslen *et al.* (1993). No atomic coordinates, lattice parameters and temperature factors of the trace phases have been refined. Only the scale factors for the three trace phases were adjusted. The results obtained for cuprorivaite from both samples are compared in Table 4. The crystal

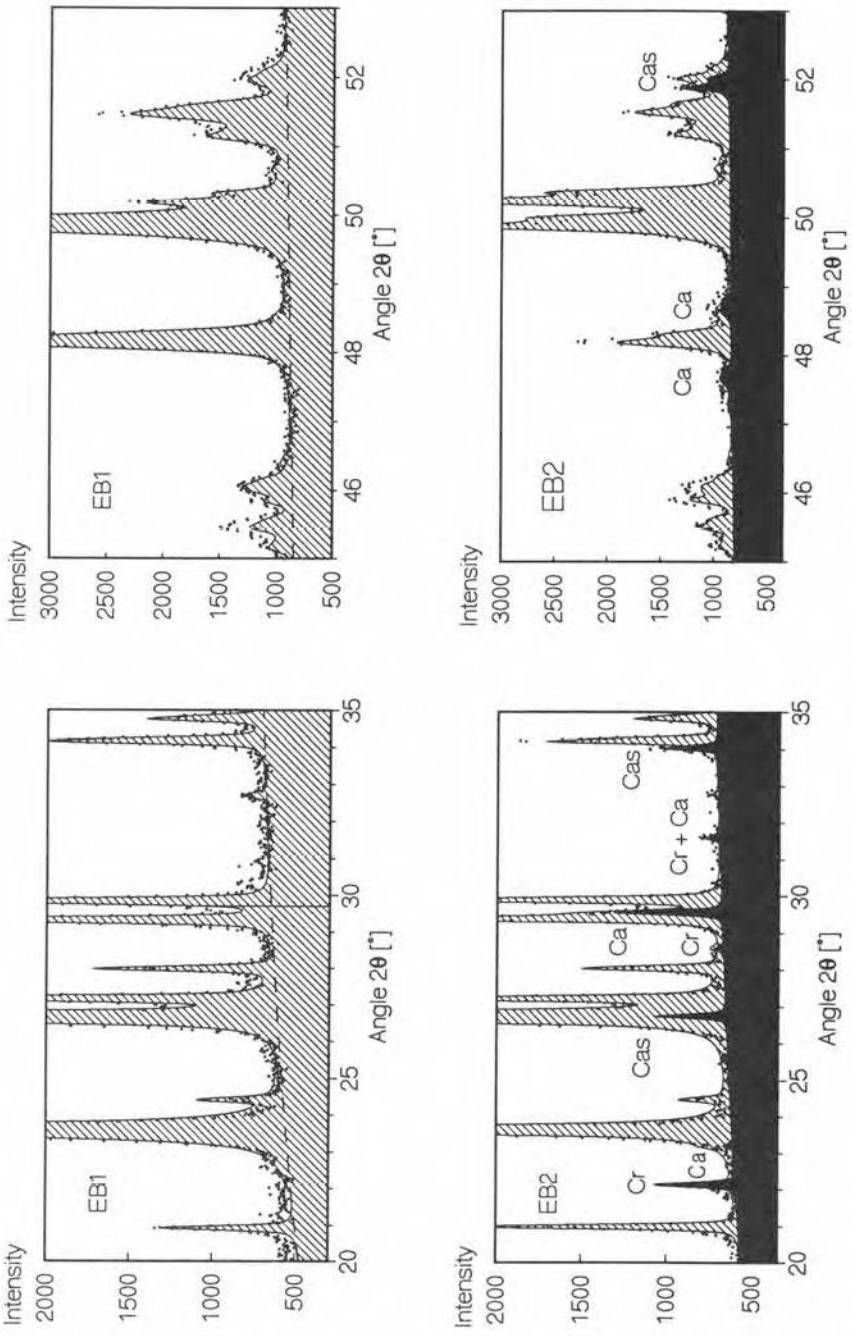

Fig. 12. Comparison of two selected regions of the powder diffractograms of Egyptian Blue samples EB1 and EB2 (dots), including the most prominent reflections of the detected trace phases. The Rietveld fit to the main phases cuprorivaite and quartz is indicated by hatched areas. The contributions of the trace phases cristobalite (Cr), calcite (Ca) and cassiterite (Cas) found in sample EB2 were fitted to the measured data by the Rietveld method and are marked by a filled black profile. Radiation was Cu-Kα.

structure data compare well to the results of Pabst (1959).

In Fig. 12 selected regions of the powder diagrams of both samples EB1 and EB2 are compared. In these regions the most prominent reflections of the trace phases detected in the sample EB2 from Qantir appear. A comparison shows that the Omani Egyptian Blue sample is free from these impurities. The contributions of the trace phases to the powder diagram of sample EB2 are marked by a filled black profile as calculated by the Rietveld refinement. Hatched reflections are

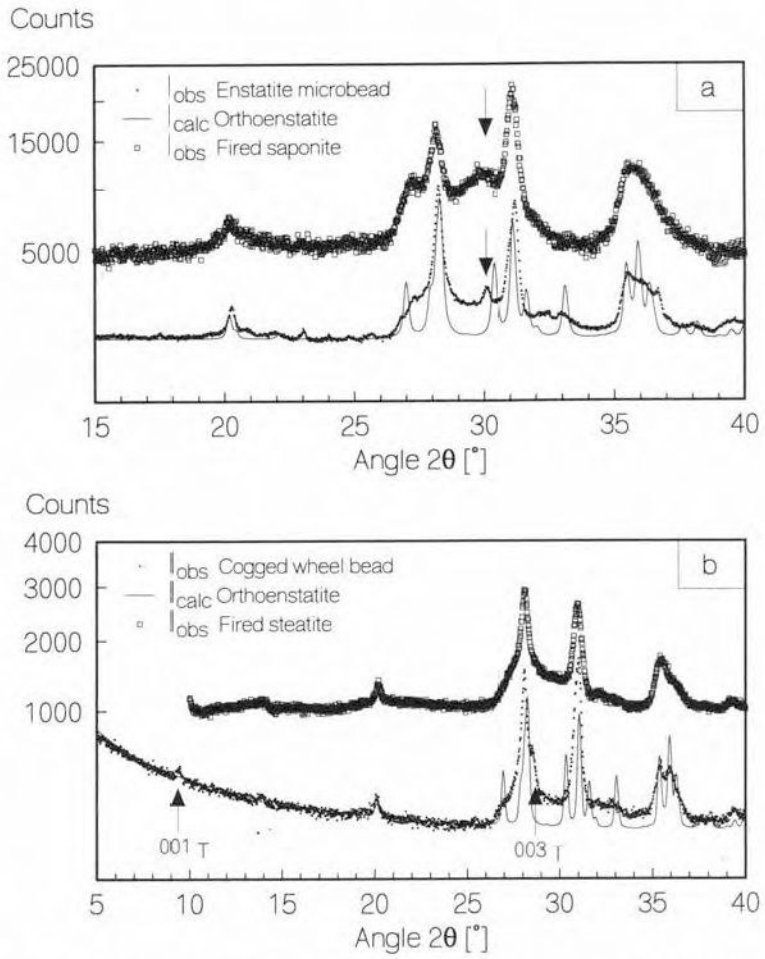

Fig. 13. **a**. X-ray powder diffractogram of Omani microbeads (dots) compared to a calculated powder diagram of well crystallized orthoenstatite (solid line) and to the powder diagram of a fired saponite sample (open squares). A reflection at 30.0° 2θ (arrows) seems to distinguish fired saponite from fired massive steatite, the latter shown in Fig. 13b. **b**. X-ray powder diffractogram of the cogged wheel bead (dots) compared to a calculated powder diagram of well crystallized orthoenstatite (solid line) and to the powder diagram of a fired massive steatite (open squares). Reflections at the positions of the talc 001 and 003 peaks (arrows) may be due to remaining untransformed raw material. Radiation was Cu-Kα.

due to the main constituents cuprorivaite and quartz. Sample EB2 from Qantir has a higher quartz content resulting in more intense quartz peaks. Another distinctive feature of the Egyptian Blue powders is the glass content observed in sample EB2.

Synthetic enstatite beads

In some graves at al Maysar which date to the Umm an-Nar Period (2700-2000 BC), thousands of whitish cylindrical beads (here microbeads) occurred (Fig. 3h). Typical bead dimensions are 5 mm in length and 2.5 - 3 mm in diameter. These may have formed entire garments. The X-ray diffraction pattern of one pulverized bead reveals an orthoenstatite-related structure. An enstatite composition was corroborated by electron microprobe analysis. For comparison with a well-crystallized orthoenstatite, a calculated powder pattern is superimposed on the X-ray pattern of the enstatite microbead in Fig. 13a. The data for

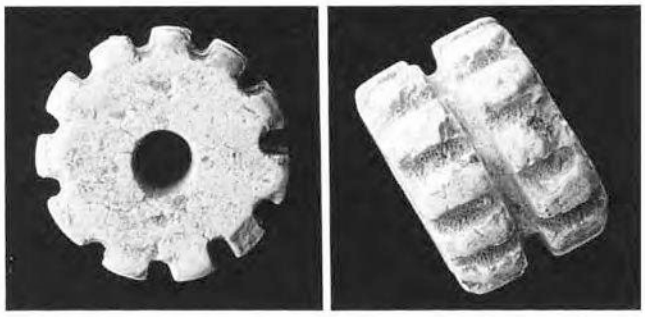

Fig 14. Synthetic enstatite bead in the shape of a cogged wheel viewed parallel and perpendicular to the threadhole axis; diameter 6.5 mm. The bead was presumably carved from a soft steatite and then fired at about 1000°C to form a phase with a structure related to enstatite.

the pattern simulation of orthoenstatite were taken from Carlson *et al.* (1988).

Crystal structures resembling enstatite are formed from Mg-silicates like talc or clay minerals such as Mg-rich smectites *via* a topotactic phase transformation at temperatures above 700° to 1000°C (Evans & Guggenheim, 1985). Therefore, a heating experiment on Mg-rich clay (saponite) was carried out to compare powder diffractograms of the bead and the fired clay. The saponite sample was fired for 24 hours at 1000°C and transformed into a phase with a crystal structure related to orthoenstatite. The powder diffractogram closely resembles the one from the microbead material as illustrated in Fig. 13a.

In a grave of the Samad Culture an attractive, whitish, short, cylindrical bead in the form of a cogged wheel came to light. Due to the details of its construction and the fine material it was presumably fabricated far earlier. This bead, reproduced in Fig. 14, has a diameter of 6.5 mm and a height of 4.5 mm. A powder diffractogram was obtained from one of the basal planes of the cylinder. This revealed a phase with a structure which resembles enstatite. Again a calculated orthoenstatite powder pattern is superimposed in Fig. 13b. Since the bead is rather complicated in shape, it is likely that it was worked from soft steatite (talc) bulk material and then fired at about 1000°C. During this procedure the steatite transformed into orthoenstatite, and the formerly soft bead became hard and durable. To confirm this, a pure massive steatite was fired for 24 hours at 1000°C. In Fig. 13b we compare the powder diffractogram of this fired bulk sample with that of the cogged wheel bead from Oman. A good overall resemblance of the two powder patterns is evident. The powder pattern of the bead shows peaks at positions close to the 001 and 003 reflections of talc which may be due to some remaining untransformed raw material.

If one compares the diffractograms of the cogged wheel bead and the fired massive steatite on the one hand with those of the synthetic enstatite microbead and the fired saponite on the other hand, a peak at 30.0° 2 θ in diffractograms of the second group occurs as a distinctive feature (Fig. 13a). This sheds some light on the raw material used.

As beads may also be produced by firing of reshaped talc powder (Hegde *et al.*, 1982), a further experiment concerning the manufacturing process for synthetic enstatite beads was conducted. Talc was pulverized, reshaped into a cylinder and then fired under the same conditions as the massive steatite. The diffractogram of this material is entirely different from powder diagrams of fired saponite and massive bulk steatite. The transformation mechanism and therefore the resulting enstatite-like structure and the details of the powder diagrams of the newly produced enstatite may depend on the state of crystallinity of the raw material. Textures present in massive steatite may significantly influence the details of the transformation from talc to enstatite. Recently, structural changes induced in talc by dry grinding were observed by Aglietti (1994). Further studies are necessary to clarify whether the differences observed in the enstatite powder diagrams are replicable features indicative of the raw material and the manufacturing process of the beads.

Discussion of archaeological aspects

Beads form an important group of archaeological finds of different cultures and periods. Nonetheless, archaeometrical investigations have rarely been carried out on beads in general and never on beads from ancient Oman and Sri Lanka. X-ray powder diffraction and electron microprobe analysis provide detailed information on the material of the beads. This information in part gives some answers to certain archaeological problems.

Beads made from ultramafic rocks: The material of these beads compares well with vessels and small items made from chloritite which came to light at several locations in Oman and were produced from the mid-third millennium BC onward. An archaeological and mineralogical description of these finds is given by David *et al.* (1990). The chlorites detected in these objects are also clinochlore/sheridanite and ripidolite (Fig. 4). Source rocks for the raw material are chloritites which occur in numerous small outcrops of black-wall sequences along the contact between peridotitic and gabbroic rocks from obducted oceanic mantle and crust, respectively, within the large Samail Ophiolite of Oman. In these outcrops, chloritites with identical chlorite compositions were found (David *et al.*, 1990). One outcrop is situated close to the Samad oasis. Usually, outcrops of black-wall sequences also contain serpentinites and massive chlorite-amphibole rocks. Thus it is very likely that the beads made from ultramafic rocks were produced in the Samad region from locally available raw materials.

Garnet beads: The rather homogeneous compositions of the nine beads from Samad allow the conclusion that all such beads derive from the same source material. Garnets with this composition and of gemstone quality do not occur in any of the rock sequences of Oman. The only garnets known there are from eclogites intercalated within the ophiolite series (El Shazly *et al.*, 1990). These garnets are small (< 1 mm), tectonically sheared and broken, and their chemical composition differs clearly from that of the beads (Fig. 6). Thus either the beads or the raw material are imports to Oman. The composition of garnet beads from Oman closely matches that of garnet beads from Tissamaharama. Therefore, most likely the garnet beads at Samad were imported from Sri Lanka or India. This supports the archaeological hypothesis of intensive ancient trade connections between central Oman and the India/Sri Lanka areas (Yule, 1994).

Glass beads: Comparative investigation of glass beads from Samad and Tissamaharama was prompted by the close chemical resemblance of garnet beads and the stylistic similarity of certain glass beads from both excavations. Up to now, no common chemical features could be detected for glass beads from Samad and Tissamaharama.

For reddish-brown glass beads from both locations, completely different compositions and manufacturing processes have been recognized. The beads from Samad are Na-dominated, sometimes contain Pb, and are coloured by Cu dissolved in the glass matrix. As shown by relics of Cu_2S, Cu-sulphides were used as raw material for a Cu-addition to the melt, probably after sulphide roasting. This may point to a local production of these beads in Oman, where Cu-sulphide exploitation has been carried out over the last 5000 years (Hauptmann, 1985).

Reddish-brown beads from Tissamaharama are K-pronounced and contain densely dispersed Cu_2O droplets. These opaque red glasses are known from the 2nd millennium BC on. The bright, sealing-wax redbrown colour results from the cuprite particles which crystallize from the Cu-saturated glass matrix when the melt is cooled down for nucleation and then tempered. Depending on the time and temperature of heat treatment, the morphology of the cuprite crystals changes from droplets to cubes and finally skeletal or dendritic forms. (Ram *et al.*, 1969; Ahmed & Ashour, 1981; Bimson, 1987; Harding *et al.*, 1989). The opaque red glass of the Tissamaharama beads differs from most other comparable red glasses by a complete lack of PbO.

Sandwich beads from both localities differ mainly in the chemical composition of the white interlayers. In beads from Samad, these layers generally contain a remarkably high content of SnO_2 as opacifier, which is completely missing in the white layer of a sandwich bead from Tissamaharama. On the other hand, CaO- and P_2O_5-rich patches have been found in some of the reddish-brown glass beads and in the sandwich bead from Tissamaharama but never occur in glass beads from Samad.

Synthetic enstatite beads: By virtue of our data it seems reasonable that the enstatite cogged wheel bead was produced from steatite and, after cutting, was hardened by firing at around

1000°C. The firing transforms the steatite to enstatite. Geologically, steatite often occurs together with chloritite and serpentinite in black-wall sequences. Thus, the raw material of the examined bead may have a common origin with the ultramafic black-wall rocks of the Oman Samail Ophiolite used for local bead production.

On the other hand, the cogged wheel bead and the microbeads again may be taken as an indication of ancient connections to India. With regard to beads, the Indus Civilization is described as a "steatite civilization" (Vats, 1940). A typical group of beads from this civilization was defined by various terms such as "white steatite", "burnt steatite", "reformed steatite", "glazed steatite" or "paste". The problem of the manufacturing process of "paste" beads was recently discussed by Vidale (1989). These beads are believed to be made of fired steatite, similar to the cogged wheel bead from the Samad grave. In context with the Indian "paste" beads, a find of thousands of microbeads in a male burial at Harappa (Fig. 1) was reported.

Hundreds of similar beads were recently found at Jebel al Emalah (United Arabian Emirates) in a grave dated in the Umm an-Nar period (Benton, 1994). It is assumed that these beads were used as ornamentations sewn onto clothing.

Conclusions

Our data of beads from Oman and Sri Lanka and the discussion of archaeological aspects show that investigation of archaeological finds by means of archaeometrical methods can result in answers to archaeological problems. It is of course not possible to clearly answer every question. In many cases, however, a detailed characterization of the material can support or disprove ideas about the production method or the provenance of archaeological finds. Often, a severe handicap in archaeometry is the lack of representative data on the materials of different archaeological finds from various regions for comparative studies. Most finds have never been the subject of archaeometrical investigations. One reason is that the objects must be destroyed to a certain degree for measurements. If archaeometry aims to generate a wide data base for comparative studies, non-destructive methods for analysis have to be used more extensively.

Using an electron microprobe, objects such as garnet beads, gold beads or certain glass beads could be analyzed in a wholly non-destructive way, but nonetheless with accurate results. Beads made from ultramafic rocks or slightly corroded glass beads were measured nearly non-destructively after a soft and inconspicuous polishing to remove a thin patina. Electron microprobe measurements in many cases could allow investigation of precious and unique finds. The method is also very suitable for analyzing a complete series of similar objects from one find to get statistically sounder informations about their chemical variability. For some time archaeometallurgists have used electron microprobe analysis as a well established method for their investigations. It is desirable that nearly or even completely non-destructive microprobe analysis will be used as a common tool for systematic work on various archaeological objects like beads, seals, small fibulas or coins.

X-ray powder diffraction is commonly used in archaeometry as a destructive method, often for the investigation of ancient ceramics. As a non-destructive method it was applied only sporadically, for example to identify colouring pigments in art objects (*i.e.* Fuchs, 1995). Our results show that the method is suitable for different kinds of small objects with a flat surface or a surface that is not too irregular. Non-destructive X-ray powder diffraction could be used much more extensively for systematic investigations of polycrystalline archaeological finds.

Acknowledgements: We thank Gerd Weisgerber from the German Mining Museum in Bochum and Ali Shanfari of the Department of Antiquities in Muscat for providing unrestricted access to the extensive bead complex of the excavations in the Sultanate of Oman and for their very friendly help during the sampling of representative beads for our investigations. Hans-Joachim Weisshaar from the Commission of General and Comparative Archaeology in Bonn who leads the excavations in Tissamaharama is thanked for his support of our study. Siran Deraniyagala and W. Wijeyapala from the Archaeological Department of Sri Lanka are thanked for fruitful cooperation. Heidrun Schenk decisively attributed to the discussion about stratigraphy and chronology. Photographs were taken by Klaus-Peter Kelber, Willibald Böhm kindly undertook the construction of special sample mounts, and Peter Späthe is responsible for part of the sample preparation. Stani Ulitzka, Martin Okrusch, Ingrid Abs-

Wurmbach and an anonymous reviewer are thanked for critically reading the manuscript. The Industrie- und Handelskammer Würzburg/Schweinfurt kindly financed the acquisition of the software JADE+ for phase analysis from powder diffraction data. Finally, the financial support of Deutsche Forschungsgemeinschaft (grant Ho 1714/1-1) is gratefully acknowledged.

References

Aglietti, E.F. (1994): The effect of dry grinding on the structure of talc. *Appl. Clay Sciences*, **9**, 139-147.

Abdelouas, A., Crovisier, J.L., Lutze, W., Müller, R., Bernotat, W. (1995): Stucture and chemical properties of surface layers developed on R7T7 simulated nuclear waste glass altered in brine at 190°C. *Eur. J. Mineral.*, **7**, 1101-1114.

Ahmed, A.A. & Ashour, G.M. (1981): Effect of heat treatment on the crystallisation of cuprous oxide in glass. *Glass Technology*, **22**, 24-34.

Baur, W.H. (1956): Über die Verfeinerung der Kristallstrukturbestimmung einiger Vertreter des Rutiltyps: TiO_2, SnO_2, GeO_2 und MgF_2. *Acta Cryst.*, **9**, 515-520.

Benton, J. (1994): Recent excavations at Jebel al Emalah (U.A.E.). *Orient Express*, **1994/1**, 17-18.

Bimson, M. (1987): Opaque red glass: A review. *in* "Early Vitreous Materials", M. Bimson & I.C. Freestone, ed. British Museum Occasional Paper 56, London.

Brindley, G.W. (1980): Order-disorder in clay mineral structures. *in* "Crystal structures of clay minerals and their x-ray identification", G.W. Brindley & G. Brown, ed. Mineral. Soc. Monogr. No. 5, London, 125-196.

Carlson, W.D., Swinnea, J.S., Miser, D.E. (1988): Stability of orthoenstatite at high temperature and low pressure. *Amer. Mineral.*, **73**, 1255-1263.

David, H., Tegyey, M., Le Metour, J., Wyns, R. (1990): Les vases chloritite dans la péninsule d'Oman: une étude pétrographique appliquée à l'archéologie. *C. R. Acad. Sci. Paris*, **311/II**, 951-958.

El Shazly, A., Coleman, R.G., Liou, J.G. (1990): Eclogites and blueschists from northeastern Oman: Petrology and P-T evolution. *J. Petrol.*, **31**, 629-666.

Evans, B.W. & Guggenheim, S. (1985): Talc, pyrophyllite, and related minerals. *in* "Hydrous Phyllosilicates", S.W. Bailey, ed. Mineral. Soc. America., Reviews in Mineralogy 19, 225-294.

Fuchs, R. (1995): Zerstörungsfreie Röntgendiffraktometrie - Kunstwerke im Röntgenstrahl. *Archäometrie und Denkmalpflege - Kurzberichte*, **1995**, 101-104.

Grauby, O., Petit, S., Decarreau, A., Baronnet, A. (1993): The beidellite-saponite series: an experimental approach. *Eur. J. Mineral.*, **5**, 623-635.

—, —, —, — (1994): The nontronite-saponite series: an experimental approach. *Eur. J. Mineral.*, **6**, 99-112.

Harding, R.R., Hornytzkyj, S., Date, A.R. (1989): The composition of an opaque red glass used by Fabergé. *J. Gemm.*, **21**, 275-287.

Hauptmann, A. (1985): 5000 Jahre Kupfer im Oman. Bd.I: Die Entwicklung der Kupfermetallurgie vom 3. Jt. bis zur Neuzeit. *Der Anschnitt*, **Beih.4**, 137 p.

Hegde, K.T.M., Karanth, R.V., Sychantavong, S.P. (1982): On the Composition and Technology of Harappan Microbeads. *in* "Harappan Civilization", G.L. Possehl, ed. New Delhi, 239-244.

Hey, M.H. (1954): A new review of the chlorites. *Mineral. Mag.*, **30**, 277-292.

Hill, R.J. & Howard, C.J. (1986): A Computer Program for Rietveld Analysis of Fixed Wavelength x-ray and Neutron Powder Diffraction Patterns. Australian Atomic Energy Commission, (AAEC) **M112**, Sutherland, 15 p.

Jaksch, H. (1985): Farbpigmente aus Wandmalereien altägyptischer Gräber und Tempel: Technologien der Herstellung und mögliche Herkunftsbeziehungen. Dr.rer.nat.-Thesis, Ruprecht-Karls Universität, Heidelberg, 240 p.

Leake, B.E. (1978): Nomenclature of amphiboles. *Amer. Mineral.*, **98**, 1023-1052.

Le Page, Y. & Donnay, G. (1976): Refinement of the crystal structure of low quartz. *Acta Cryst.*, **B32**, 2456-2459.

Maslen, E.N., Streltsov, V.A., Streltsova, N.R. (1993): X-ray study of the electron density in calcite, $CaCO_3$. *Acta Cryst.*, **B49**, 636-641.

Noll, W. (1981): Zur Kenntnis altägyptischer Pigmente und Bindemittel. *N. Jb. Mineral. Mh.*, 416-432.

— (1991): Alte Keramiken und ihre Pigmente. E. Schweizerbart'sche Verlagsbuchhandlung, Stuttgart, 334 p.

Pabst, A. (1959): Structure of some tetragonal sheet silicates. *Acta Cryst.*, **12**, 733-739.

Pawley, G.S. (1981): Unit cell refinements from powder diffraction scans. *J. Appl. Cryst.*, **14**, 357-361.

Pluth, J.J., Smith, J.V., Faber, J. (1985): Crystal structure of low cristobalite at 10, 293, and 473 K: Variation of framework geometry with temperature. *J. Appl. Phys.*, **57**, 1045-1049.

Ram, A., Prasad, S.N., Srivastava, K.P. (1969): New conception on the origin of colour in copper ruby glass. *Sprechsaal für Keramik, Glas, Email, Silikate*, **102**, 315-320.

Rapson, W.S. (1990): The metallurgy of the coloured carat gold alloys. *Gold Bull.*, **23**, 125-133.

Restori, R. & Schwarzenbach, D. (1986): Charge density in cuprite, Cu_2O. *Acta Cryst.*, **42**, 201-208.

Rösch, C. (1994): Präislamische Schmuckperlen aus dem Sultanat Oman - mineralogisch-materialkundliche Untersuchungen. Diplom-Thesis, Univ. Würzburg, 211 p.

Sellner, C., Oel, H.J., Camara, B. (1979): Untersuchung alter Gläser (Waldglas) auf Zusammenhang von Zusammensetzung, Farbe und Schmelzatmosphäre mit der Elektronenspektroskopie und der Elektronenspinresonanz (ESR). *Glastechn. Ber.*, **52**, 255-264.

Sigurdsson, H., D'Hondt, S., Arthur, M.A., Bralower, T.J., Zachos, J.C., van Fossen, M., Channell, J.E.T. (1991): Glass from the Cretaceous/Tertiary boundary in Haiti. *Nature*, **349**, 482-487.

Strese, H. & Hofmann, U. (1941): Synthese von Magnesiumsilikat-Gelen mit zweidimensional regelmäßiger Struktur. *Z. Anorg. Allg. Chem.*, **247**, 65-95.

Tite, M.S., Bimson, M., Cowell, M.R. (1984): Technological examination of Egyptian Blue. *in* "Archaeological Chemistry - III", J.B. Lambert, ed. American Chemical Society, Washington, 215-242.

Vats, M.S. (1940): Excavations at Harappa. New Delhi.

Vidale, M. (1989): Early Harappan Steatite, Fayence and Paste Beads in a Necklace from Mehrgarh-Nausharo (Pakistan). *East & West*, **39**, 291-300.

Weisshaar, H.-J. & Wijeyapala, W. (1993): Ancient Ruhuna (Sri Lanka), the Tissamaharama Project: Excavations at Akurugoda 1992-1993. *Beiträge zur Allgemeinen und Vergleichenden Archäologie*, **13**, 127-166.

—, — (1994): The Tissamaharama Project 1992-1993 (Sri Lanka): Metallurgical remains of the Akurugoda Hill. *South Asian Archaeology*, **1993**, 803-814.

Wiles D.B. & Young, R.A. (1981): A new computer program for Rietveld analysis of x-ray powder diffraction patterns. *J. Appl. Cryst.*, **14**, 149-151.

Young, R.A. (1993): The Rietveld Method. Int. Union of Crystallography Monographs, Oxford University Press, 298p.

Yule, P. (1992): Samad al Shan, eine vorislamische Nekropole im Sultanat Oman. *Nürnberger Blätter zur Archäologie*, **9**, 39-48.

— (1993): Excavations at Samad Ash Shan 1987-1991, Summary. *Proc. Sem. Arab. Studies*, **23**, 141-153.

— (1994): Die Gräberfelder in Samad al Shan (Sultanat Oman). Materialien zu einer Kulturgeschichte. Habilitation-thesis, Univ. Heidelberg, 4 volumes.

This paper was presented at the "X-ray Crystallography : Progress in Methods and Applications" Symposium in Würzburg (March 1995)

Received 1 Août 1995